Proceedings of CHT-17
ICHMT International Symposium on Advances in Computational Heat Transfer

May 28-June 1, 2017, Napoli, Italy

CHT-17-203

Heat Generation in Gold Nanorods Solutions due to Absorption of Near-Infrared Radiation

Xi Gu[*,§], Victoria Timchenko[*], Guan Heng Yeoh[*,**], Leonid A. Dombrovsky[***] and Robert Taylor[*]
[*]School of Mech. & Manuf. Eng., UNSW, Sydney, NSW, Australia
[**]Australian Nuclear Science and Technology Organisation (ANSTO), Kirrawee DC, NSW, Australia
[***]Joint Institute for High Temperatures, Krasnokazarmennaya St, Moscow, Russia
[§]Correspondence author. Fax: +61 2 9663 1222 Email: xi.gu@unsw.edu.au

ABSTRACT Hyperthermia treatment of tumours surrounded by healthy tissues can be enhanced using radiative heating of embedded gold nanoparticles (GNPs) due to their optical resonance absorption in the so-called optical therapeutic window. In this paper resonance absorption of gold nanorods (GNRs) and correspondent heat generation in GNR solutions was studied both numerically and experimentally. The calculations based on the discrete-dipole approximation (DDA) showed a consistent relationship between the maximum absorption efficiency and the nanorod orientation with respect to the incident radiation. Additionally, the plasmonic wavelength and the maximum extinction efficiency of a single nanorod were shown to increase linearly with its aspect ratio when the nanorod volume was fixed. The wavelength of the surface plasmonic resonance (SPR) was found to change when the gold nanorods were closely spaced. Specifically, a shift and broadening of the resonance peak in the optical spectrum was obtained when the distance between the nanorods was about 50 nm or less. In parallel to numerical simulations, the optical experiment was performed where the transmission and reflection of suspended nanorods at various volume fractions were measured by a spectrophotometer to investigate their capability of absorption and heating. The plasmonic wavelength of the nanorods solution was shown to be around 780 ± 10 nm, which was in good agreement with computational predictions for coupled side-by-side nanorods. The temperature of solution heated by near infrared light was also measured in the laboratory experiments at various volume fractions of suspended nanorods. It was found that the rate of increase for both the temperature of solution and the absorbed light diminished when the volume fraction of suspended nanorods reached about 1.24×10^{-6}. This can be explained by partial clustering of nanorods at their high volume fractions in water.

INTRODUCTION

Potential of nanoparticle hyperthermia therapy to treat cancer diseases has been widely investigated in the last decade (Melancon et al. [2008], Huang et al. [2008], Huang and El-Sayed [2011] and Austin et al. [2014]). Because of the enhanced permeability and retention effect, GNPs conjugated to specific antibodies or other targeting ligand can easily penetrate leaky tumour blood vessels and selectively target cancerous cells. The significance of using GNPs for hyperthermia treatment arises because of their unique strong optical resonance absorption of near infrared light in the so-called optical therapeutic window that results in a controllable, rapid increase of temperature (Mackey et al. [2014], Wang et al. [2012] and Huang et al. [2006]).

As the human skin tissues can barely absorb light with a wavelength between 700 nm to 900 nm, near infrared (NIR) light can be applied to optically penetrate biological tissues and thus to irradiate suitable GNPs injected inside superficial tumours (Bashkatov et al. [2005]). As the peak of this resonance absorption can be tuned depending on the size and shape of GNPs, Loo et al. [2005], Melancon et al. [2008], Huang et al. [2009] and Huang and El-Sayed [2010] have explored different types of GNPs including nanospheres, nanoshells and nanorods. The latest have been shown to be particularly effective for heating of the tissues due to their relatively strong plasmonic resonance (SPR) in the near infrared spectral range within an optical tissue window. According to Jain et al. [2006], the calculated SPR absorption efficiency of gold nanorods were much higher than nanospheres and nanoshells. Additionally, the SPR of nanorods could be highly controllable by modifying their aspect ratio. Cai et al. [2008] explained that due to the complicated structure of nanoshells, manufacturing nanorods were rather easier than producing nanoshells. However, the effects of nanorod orientation and possible electromagnetic interaction between the closely spaced nanorods on the plasmonic absorption have not been quantitatively studied yet. As was shown by Nikoobakht et al. [2000], Caswell et al. [2003] and Sun et al. [2008], the volume fraction of the solution can result in preferred orientation or self-assemblies of gold nanorods (GNR). Also, Jain and El-Sayed [2008] calculated that the aggregation of gold nanorods can cause a significant shift of the surface plasmonic resonance (SPR) wavelength of gold nanorod. Since the heating ability of gold nanorods highly depends on their optical properties, the heat generation in GNRs solutions of a certain concentration can be possibly affected by the effects of the self-assemblies. However, the impact of various concentrations on the optical properties and the heat ability of GNR solutions when the solutions are exposed to a light source have not been analysed. The current paper explains the in-depth cause of the varying heating capability of GNR solutions using both computational and experimental methods. Discrete dipole approximation (DDA) based on Mie theory was applied to calculate the optical properties of a single GNR and GNR dimers with various gaps within the assemblies. In parallel, the optical experiment was performed where the transmission and reflection of suspended nanorods at various volume fractions were measured to investigate their capability of absorption. The numerical predictions have been compared with the optical experimental results to obtain a comprehensive understanding of the effects of nanorods orientation and their aggregation. The temperature increase of solutions exposed to near infrared light was also measured in the laboratory experiments at various volume fractions of suspended nanorods to investigate the impact of the affected optical properties on heat generation efficiency of GNR solutions which has not been investigated in previous studies.

METHODS

Optical Experiment The diameter of investigated GNR was 10 ± 1 nm and the axial length was 38 ± 3.8 nm. Thus, the aspect ratio (AR) and effective radius were around 3.8 and 8.9 nm. From the specification provided by the manufacturer, the plasmonic resonance of the GNR solution was equal to 780 nm. Both optical and thermal experiments were performed with a same batch of GNR solutions of various concentrations being used. 6 samples of water based GNR solutions were examined by a spectrophotometer. Absorbance of the samples was calculated using the following equation:

$$A = \log_{10}\frac{P}{P_0} = 2 - \log_{10}(T \times 100) \quad (1)$$

where A and T were the absorbance and measured transmittance of the samples, P was the light intensity the sample received and P_0 was the light intensity transmitted through the samples.

The volume of each sample was $1 \times 1 \times 3.5$ cm^3. The concentration shown in Table 1 indicates the number of GNRs per millimetre. Sample A contained pure water while Sample F had GNR solution purchased from Sigma-Aldrich in which according to the specification sheet provided by the manufacturer, the every millimetre solution contained at least 30 μg of gold. In samples B, C, D and

E, the same GNR solution was diluted by different amount of water to obtain different concentrations/volume fractions of GNRs (see Table 1 below). It should be noted that the use of water as a host medium leads to the radical simplification of the radiative transfer problem. The radiation is not scattered in pure water and the scattering of NIR radiation by suspended nanoparticles is also negligible. On the contrary, all human tissues are strongly scattering media in the therapeutic window. As a result, the propagation of radiation in human tissues with embedded nanoparticles is much more complicated (Dombrovsky et al. [2011]).

Table 1
Description of GNRs Solution Samples with Various Volume Fractions

Sample	Concentration (GNRs/ml)	Volume Fraction
A	0	0
B	1.04×10^{11}	0.31×10^{-6}
C	2.08×10^{11}	0.62×10^{-6}
D	3.12×10^{11}	0.93×10^{-6}
E	4.16×10^{11}	1.24×10^{-6}
F	5.20×10^{11}	1.55×10^{-6}

Thermal Experiment In the thermal experiment, Samples D, E and F were used because the temperature increase in the samples with low concentration was not significant. For the light source the Hydrosun ® 750 lamp was used with an FB780-10 bandpass filter. The bandpass filter, which had nearly 60% transmission at 780 nm wavelength, was applied to provide a plasmonic resonance of GNRs in the optical window of biological tissues. The specific light intensity of the Hydrosun ® 750 lamp was previously analysed by present authors (Dombrovsky et al. [2015]). The sample was wrapped by Supperwool and then reflective tape to ensure the insulation and to limit the error of the experiment. The surrounding area of the sample was not exposed to the light source to prevent heating from the sides. Thermocouples were applied to continuously measure local temperature at two locations inside the samples. The averaged value of temperature increase at measured locations after a 300 seconds' exposure to the filtered light source is presented in Table 2.

Numerical Methodology Discrete dipole approximation (DDA) introduced by DeVoe [1964] has been considered as one of the most flexible and reliable method for calculating the optical properties of particles with arbitrary geometries. By using this approximation, the target is replaced by an array of point dipoles (polarisable points). The electromagnetic scattering problem for an incident periodic wave interacting with this array of point dipoles is then solved essentially exactly. In the current study, a DDA code named DDSCAT 7.3 was applied to calculate the absorption and scattering efficiency of gold nanorods. Draine and Flatau [1994] developed and validated the DDSCAT code based on Mie theory. A detailed explanation of Mie theory can be found in the book (Dombrovsky and Baillis [2010]). Lee and El-Sayed [2005], Pérez-Juste et al. [2005], Vartia et al. [2016] and Jain et al. [2006] have adopted this code to analyse optical properties of gold nanoparticles and assemblies thus the numerical method was reliable.

In DDSCAT, the size of the target is characterised by the "effective radius" to calculate the arbitrary geometry. The effective radius r_{eff} equals the radius of a sphere, which has an equivalent volume *V*.

$$r_{eff} = \sqrt[3]{\frac{3V}{4\pi}} \tag{2}$$

Since the solution was water based, the refractive index of water, $1.33 + 0i$, was applied as the refractive index of the ambient at all wavelengths. McPeak et al. [2015] measured the values of the complex dielectric function of gold at various wavelengths using a thin film of gold. However, when the target dimension was smaller than the mean free path length of electrons in the bulk material, the limitations to electron collisions within the particle would change the dampening constant of conduction electrons. This would result in size-dependent dielectric constants which are different from the dielectric constants of the bulk material. Vollmer and Kreibig [1995] developed a model to modify the real and imaginary components of the dielectric constant. This size effect need be considered and the complex dielectric function measured by McPeak et al. [2015] need be modified in the current case.

The real and imaginary components of the bulk dielectric constant ε_{bulk} can be calculated using the refractive index of the bulk material:

$$\begin{aligned} \varepsilon_r &= n^2 - k^2 \\ \varepsilon_i &= 2nk \end{aligned} \tag{3}$$

where *n* is the index of refraction and *k* is the index of absorption.

The modified dielectric constant can be expressed as:

$$\varepsilon_m = \varepsilon_{bulk} + \omega_p \frac{1}{\omega^2 + i\omega\gamma_{bulk}} - \omega_p \frac{1}{\omega^2 + i\omega\gamma_{eff}} \tag{4}$$

where ω was the frequency of the incident electromagnetic wave. According to Ordal et al. [1985], the value of bulk plasmon frequency ω_p was taken as 9.03 eV and the relaxation frequency of the bulk material γ_{bulk} as 0.072 eV. The effective relaxation frequency, γ_{eff}, can be expressed as:

$$\gamma_{eff} = \gamma_{bulk} + \frac{A_s v_f}{l_{eff}} \tag{5}$$

where the value of the Fermi velocity v_f is equal to 1.4×10^6 m/s and the value of the surface scattering parameter A_s is equal to 0.3 (Novo et al. [2006]). The effective mean free path $l_{eff,}$ was taken to be equal to the length of GNR.

RESULTS AND DISCUSSION

Experimental Results For gold nanorods the plasmon absorption splits into two bands corresponding to the oscillation of the free electrons along and perpendicular to the long axis of the rods (Devaty and Sievers [1985] and Perenboom et al. [1981]). The transverse mode shows a resonance at about 520 nm, while the resonance of the longitudinal mode is red-shifted and strongly depends on the aspect ratio (AR defined as the ratio of the length to width of the rod) of the nanorods. The presence of these two modes can be clearly observed in the results for the absorbance at 520 nm and 780 nm measured in the optical experiment and shown in Figure 1. The black line in Figure 1 indicates the maximum of absorbance depending on wavelength which slightly shifts to the red spectrum. As known from the literature (Jain and El-Sayed [2008]) a red shift of the wavelength of the SPR occurs due to aggregation of nanoparticles. So that a slight red shift in longitudinal SPR (see Figure 1) can be attributed to GNR aggregations, formed with the increase of volume fraction

of GNRs. It should be noted that the increase of absorbance diminishes with the increase of concentration of GNRs in the solution with reference solution (Sample F). The difference of absorbance between Sample E and Sample D was 0.19, while the increase of absorbance in Sample F was 0.16. These results suggested that for medical treatment an appropriate volume fraction of GNRs should be identified and applied to generate necessary amount of heat to prevent injecting too much gold. Therefore, it is important to quantify the relationship between the capability of heat generation and the volume fraction of gold nanorods solutions.

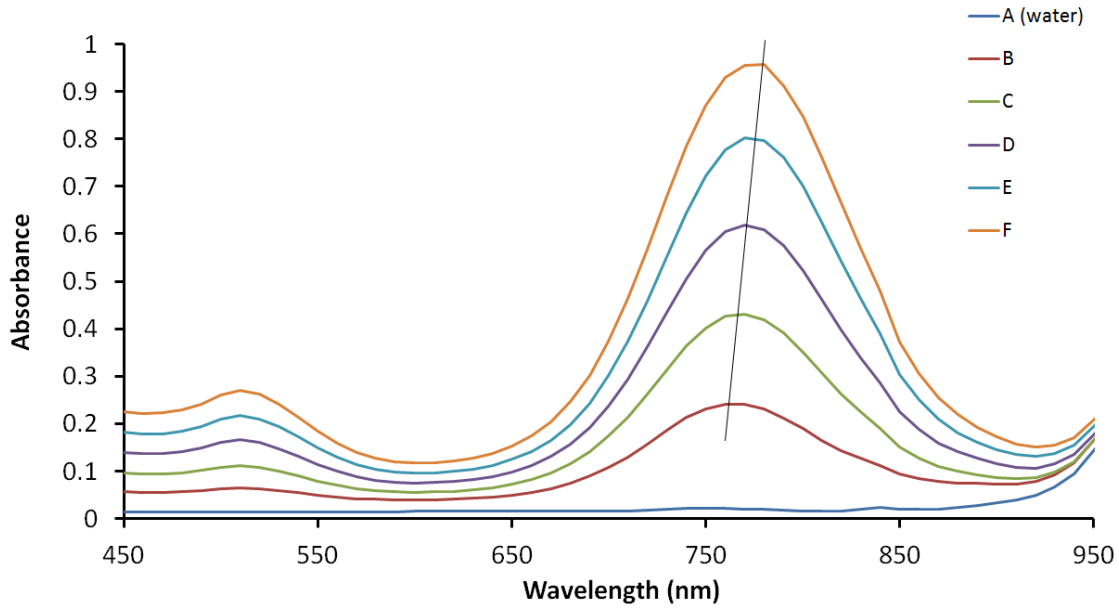

Figure 1. Absorbance of different samples in the optical experiment.

Table 2 shows the results of absorbance and temperature increase in the solutions of the optical and thermal experiments obtained at 780 nm wavelength. The averaged values of local temperature increases were recorded after a 300 seconds' exposure to the filtered light source. The values presented in Table 2 for the temperature increase are the differences between the increase in each sample and the temperature increase in the Sample A (pure water) which was 0.051 K. A correlation with absorbed intensity measured in the optical experiment can be seen in Table 2. When the volume fraction of GNRs in the samples changes from 0.93×10^{-6} to 1.24×10^{-6}, both the absorption and heat generation show obvious increases. In Sample E the absorbance increased by 0.19 causing temperature increase 0.25 degree higher than in the solution with lower concentration, whereas in Sample F the absorbance increased by 0.16 causing temperature increase 0.1 degree higher than in Sample E. One possible reason of the insignificant increase of temperature in Sample F could be that there were more light scattered by Sample F than by Sample E. The results of the optical and thermal experiments confirm that the heat generated in the solutions depends on the light energy which could be potentially absorbed by the GNRs. As can be seen from Table 2 in sample E the temperature increase is by around 0.42 degree which is only 0.09 degree lower than in the reference solution (Sample F). GNRs solution with a volume fraction of 1.24×10^{-6} therefore is the most appropriate solution in this case, because it can generate a similar amount of heat as the reference solution, with less material which is beneficial in terms of cost and possible toxicity.

Table 2
Results from Optical and Thermal Experiments Obtained at 780 nm Wavelength

Sample	Absorbance	Temperature Increase (K)
D	0.61	0.1676
E	0.80	0.4178
F	0.96	0.5102

Numerical Predictions Discrete dipole approximation (DDA) was applied to calculate the optical properties of a single GNR and GNR dimers. The optical properties of a single GNR highly depend on the angle (α) between its optical axis and the propagation direction of the light. Figure 2 presents the calculated absorption efficiency of a single AR = 3.8 GNR at various orientations. As can be seen from Figure 2, the wavelength of longitudinal SPR of the single GNR is around 800 nm and does not change with the angle. The wavelength of the transverse SPR is around 500 nm, which is same as the value obtained in the experiment. The dash line in Figure 2 indicates the average absorption efficiency of GNR at different orientations. The highest absorption efficiency was achieved when the axis of GNR was perpendicular to the incident light. However, the absorption efficiency at the wavelength of longitudinal SPR (around 800 nm) was nearly 0, when the axis of GNR was parallel to the incident light. The magnitude of transverse SPR was less than 1 so it was insignificant compared to the longitudinal SPR. Although the GNR showed a high absorption efficiency at the wavelength of longitudinal SPR, the orientations of the GNRs suspended in water can cause the absorption efficiency vary from 12 to nearly 0.

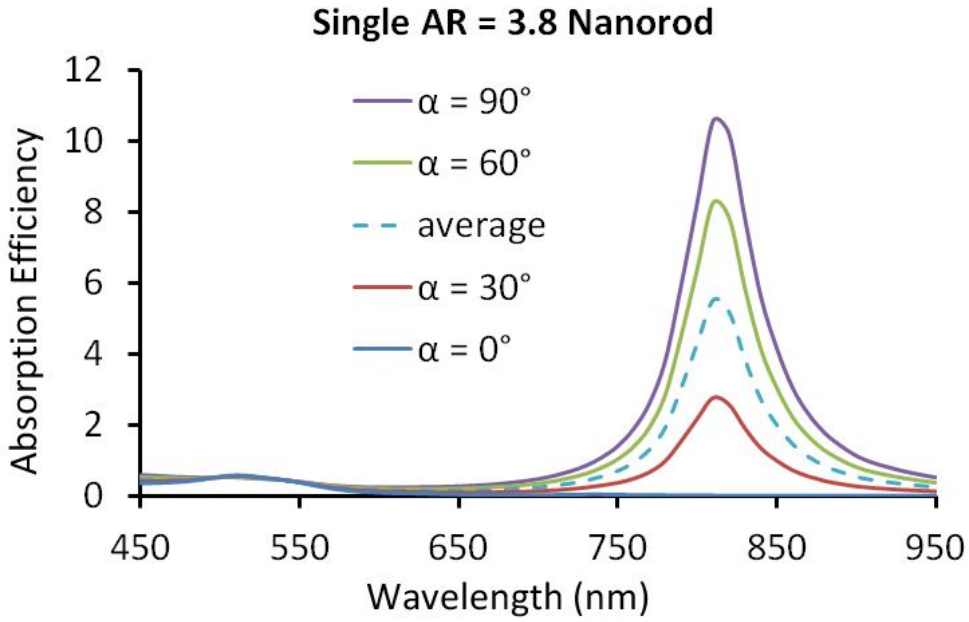

Figure 2. Spectral dependency of absorption efficiency of a single GNR

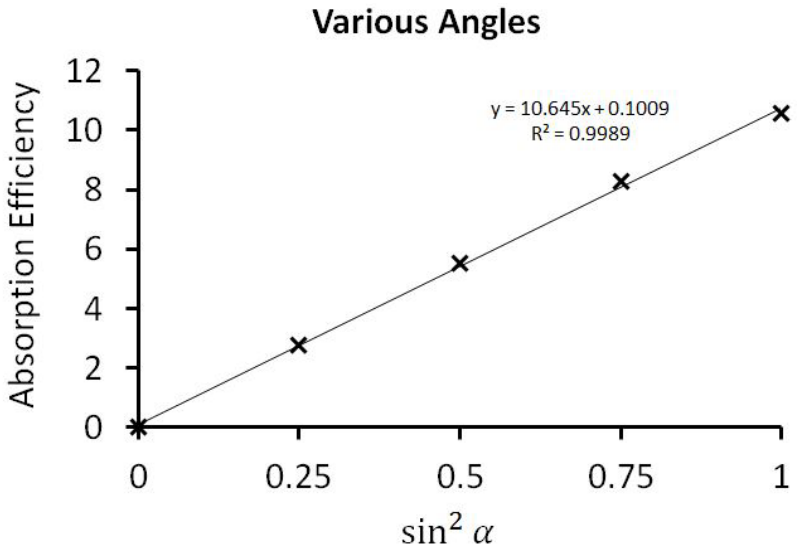

Figure 3. The linear relationship between the absorption efficiency and the orientation.

Figure 3 shows the linear relationship between the absorption efficiency and $\sin^2 \alpha$ of the GNR. The absorption efficiency of 5 different orientations at 810 nm wavelength is presented. The predictions indicate that optical properties of GNRs highly depend on the angle between its optical axis and the propagation direction of the light source. More specifically, the highest absorption efficiency of an independent GNR occurs when the GNR is perpendicular to the propagation direction of the incident light. However, the absorption efficiency could be as low as nearly 0 when the optical axis of the GNR is parallel to the propagation direction of the light.

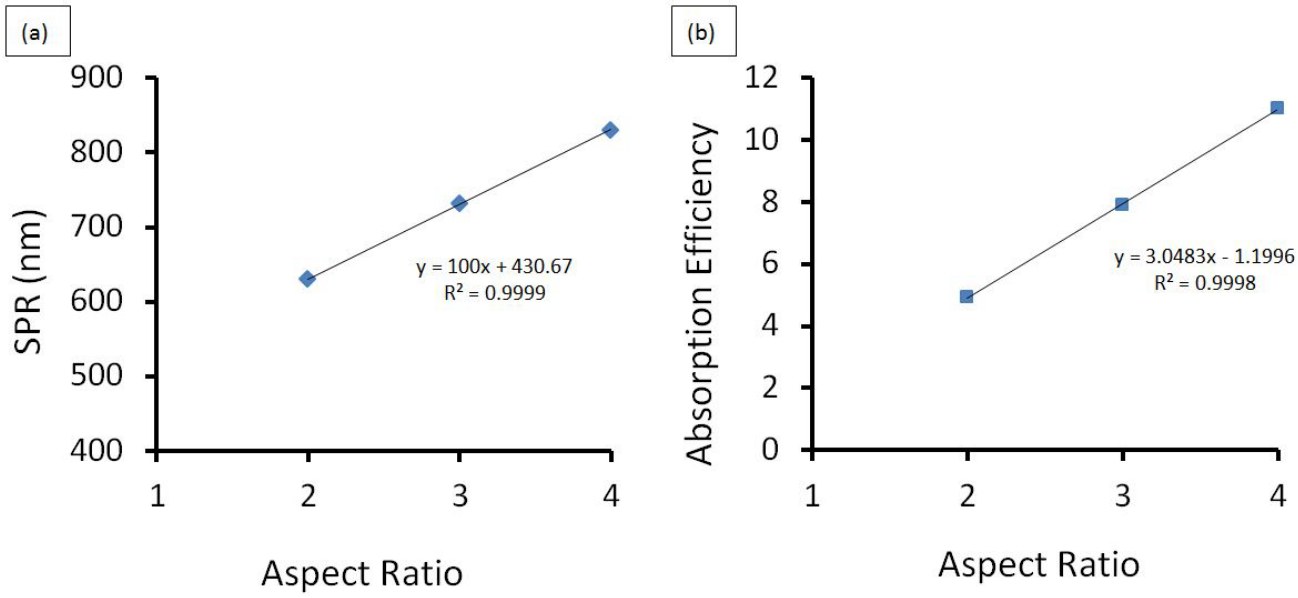

Figure 4. Linear increase of the wavelength of longitudinal SPR and of absorption efficiency with aspect ratio

As can be seen from Figure 4, the wavelength of longitudinal SPR and the extinction efficiency at this wavelength increase linearly with the aspect ratio of the GNR. Results shown in Figure 4 are obtained for perpendicular orientation of the GNR ($\alpha = 90°$) with effective radius being fixed at

8.9 nm. The wavelength of the SPR for GNR with aspect ratio AR = 3.8 calculated from linear equation shown in Figure 4 (a) is 810 nm which is the same as obtained from DDA predictions shown in Figure 2. The plasmonic resonance of absorption efficiency also showed a linear relationship with the aspect ratio as shown in Figure 4 (b). It should be noted that the absorption efficiency presented in Figure 4 (b) was obtained for each aspect ratio at correspondent SPR wavelength shown in Figure 4 (a). The wavelength of longitudinal SPR of AR = 3.8 GNR solutions measured in the optical experiment was equal to 780 nm whilst calculated using DDA method wavelength of longitudinal SPR of a single GNR was around 810 nm. This slight discrepancy between experimental and numerical results can be explained from the fact that in the numerical calculation, a single GNR in the size of exact 10×38 nm was analysed. However, the width and length of the GNRs in the solution as specified by manufacturer, could vary by up to 10% of this size, thus the aspect ratio may not be exactly 3.8 and could vary from 3.36 to 4.33. The difference could also be caused by the aggregations of GNRs in the solutions. More specifically, the wavelength of the SPR of a single GNR could vary from 700 to 1100 nm depended on the configuration as shown in Figure 5 and Figure 6 when GNR aggregations formed in the solution.

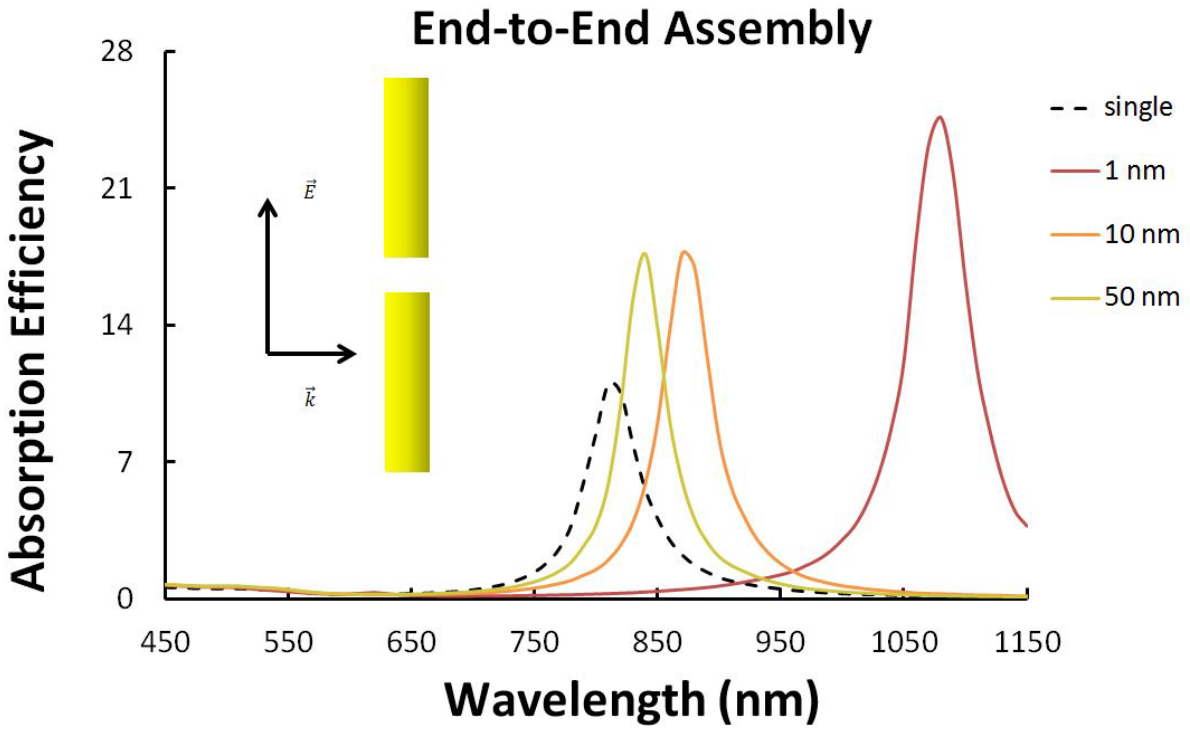

Figure 5. Absorption efficiency of end-to-end assembly with various gaps.

Figure 5 and Figure 6 present the shift in the wavelength of the SPR for two types of aggregations with various gaps between nanorods. Vector $\vec{E}$ indicates the electric field of the incident light, propagating along the $\vec{k}$ direction. In the assembly model shown in Figure 5, the GNPs were placed in end to end configuration. In the assembly model shown in Figure 6, the GNPs were located side by side. The variable distances between GNRs were used varying from 1 nm to 50 nm. As can be seen from both figures, optical properties of GNRs become almost independent and similar to a single GNR, when the distance between two nanorods is increased to 50 nm. As shown in Figure 5, the SPR of the end-to-end assembly experienced a red shift from 810 nm to over 1100 nm when the gap was 1 nm because this type of aggregation of GNRs effectively enlarged the value of aspect ratio of a single GNR which is in agreement with results predicted by Sun et al. [2008] and Jain and El-Sayed [2008]. Although the absorption efficiency of the end-to-end assembly with a small gap

was significantly higher than a single independent GNR, the longitudinal SPR wavelength was around 1100 nm, which is not within the range of the optical tissue window. Therefore, the aspect ratio of either GNRs or GNRs aggregate should not be too large.

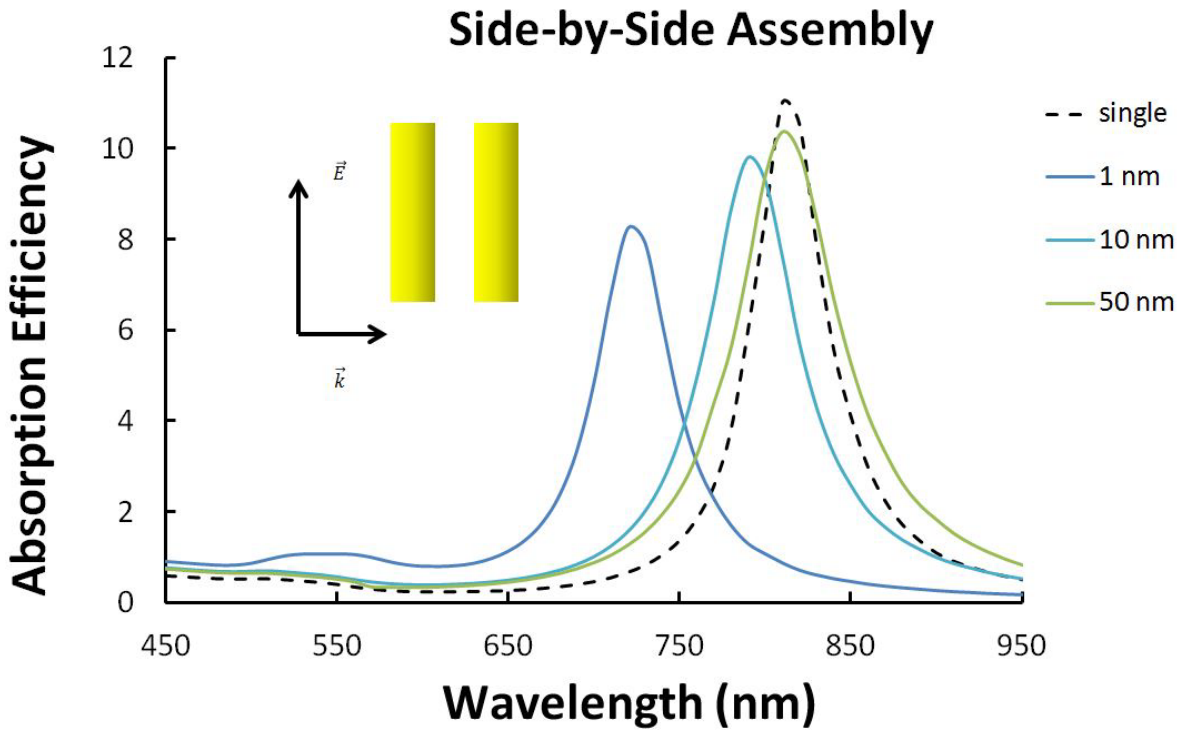

Figure 6. Absorption efficiency of side-by-side assembly with various gaps.

For side by side configuration shown in Figure 6 when the distance between GNRs was about 50 nm or less a blue shift and broadening of the resonance peak in the optical spectrum was obtained. The most significant shift was observed in particularly when the distance was smaller than 10 nm. The blue shift when the gap was shorter than 50 nm can be caused by effective decrease of aspect ratio when the side-by-side assembly is used. By analysing the experimental and numerical results shown in Figure 1, Figure 5 and Figure 6, it can be concluded that the GNRs in the samples possibly formed numerous side-by-side assemblies because the longitudinal SPR measured in the experiment was around 770 nm wavelength. With the increase of the concentration, the GNRs also formed some end-to-end assemblies, therefore a slight red shift of SPR was observed as shown in Figure 1. As potential future studies, surface treatment of GNRs and an electrical field can be applied to intentionally build similar structures of GNR aggregations for biomedical applications.

CONCLUSON

Identifying the volume fraction and particle size of GNR solution is one of the most critical tasks when irradiated GNRs are used for biomedical applications. To obtain an insight which can be useful for selection of GNR solutions, a systematic investigation of the optical properties and radiation efficiency of GNR solutions and aggregations, were undertaken for AR = 3.8 GNRs. By comparing the results of optical and thermal experiment, it was found that GNR solution with a volume fraction of 1.24×10^{-6} would be the most efficient solution because the temperature increase of the solution with this concentration was similar to the temperature increase of the solution of the higher concentration. The numerical relationship between the optical properties and the shape and the orientation of nanorods predicted by DDA can contribute to an easier and faster calculation of the optical properties of GNRs. The spectrum of end-to-end and side-by-side GNR

assemblies showed a shift and broadening of the resonance peak when the distance between the nanorods was about 50 nm or less. Moreover, when the gap was smaller than 10 nm, the SPR can shift significantly thus the heating ability of GNR solutions highly depended on the concentrations.

Acknowledgement We thank Dr. Natasha Hjerrild for preparing the samples and providing equipment applied in the optical experiments. We also appreciate Nur Amalina Omar and Dr. Felipe Crisostomo for assisting to carry out the thermal experiment.

REFERENCES

Austin, L. A., Mackey, M. A., Dreaden, E. C. & El-Sayed, M. A. [2014], The Optical, Photothermal, and Facile Surface Chemical Properties of Gold and Silver Nanoparticles in Biodiagnostics, Therapy, and Drug Delivery, *Archives of toxicology*, Vol. 88, No. 7, pp 1391-1417.

Bashkatov, A., Genina, E., Kochubey, V. & Tuchin, V. [2005], Optical Properties of Human Skin, Subcutaneous and Mucous Tissues in the Wavelength Range from 400 to 2000 Nm, *Journal of Physics D: Applied Physics*, Vol. 38, No. 15, pp 2543.

Cai, W., Gao, T., Hong, H. & Sun, J. [2008], Applications of Gold Nanoparticles in Cancer Nanotechnology, *Nanotechnology, science and applications*, Vol. 2008, No. 1, pp

Caswell, K., Wilson, J. N., Bunz, U. H. & Murphy, C. J. [2003], Preferential End-to-End Assembly of Gold Nanorods by Biotin-Streptavidin Connectors, *Journal of the American Chemical Society*, Vol. 125, No. 46, pp 13914-13915.

Devaty, R. & Sievers, A. [1985], Possibility of Observing Quantum Size Effects in the Electromagnetic Absorption Spectrum of Small Metal Particles, *Physical Review B*, Vol. 32, No. 4, pp 1951.

Devoe, H. [1964], Optical Properties of Molecular Aggregates. I. Classical Model of Electronic Absorption and Refraction, *The Journal of chemical physics*, Vol. 41, No. 2, pp 393-400.

Dombrovsky, L. A. & Baillis, D. [2010], *Thermal Radiation in Disperse Systems: An Engineering Approach*, Begell House New York,

Dombrovsky, L. A., Timchenko, V., Jackson, M. & Yeoh, G. H. [2011], A Combined Transient Thermal Model for Laser Hyperthermia of Tumors with Embedded Gold Nanoshells, *International Journal of Heat and Mass Transfer*, Vol. 54, No. 25, pp 5459-5469.

Dombrovsky, L. A., Timchenko, V., Pathak, C., Piazena, H., Müller, W. & Jackson, M. [2015], Radiative Heating of Superficial Human Tissues with the Use of Water-Filtered Infrared-a Radiation: A Computational Modeling, *International Journal of Heat and Mass Transfer*, Vol. 85, No. pp 311-320.

Draine, B. T. & Flatau, P. J. [1994], Discrete-Dipole Approximation for Scattering Calculations, *JOSA A*, Vol. 11, No. 4, pp 1491-1499.

Huang, X., El-Sayed, I. H., Qian, W. & El-Sayed, M. A. [2006], Cancer Cell Imaging and Photothermal Therapy in the near-Infrared Region by Using Gold Nanorods, *Journal of the American Chemical Society*, Vol. 128, No. 6, pp 2115-2120.

Huang, X. & El-Sayed, M. A. [2010], Gold Nanoparticles: Optical Properties and Implementations in Cancer Diagnosis and Photothermal Therapy, *Journal of Advanced Research*, Vol. 1, No. 1, pp 13-28.

Huang, X. & El-Sayed, M. A. [2011], Plasmonic Photo-Thermal Therapy (Pptt), *Alexandria Journal of Medicine*, Vol. 47, No. 1, pp 1-9.

Huang, X., Jain, P. K., El-Sayed, I. H. & El-Sayed, M. A. [2008], Plasmonic Photothermal Therapy (Pptt) Using Gold Nanoparticles, *Lasers in medical science*, Vol. 23, No. 3, pp 217-228.

Huang, X., Neretina, S. & El-Sayed, M. A. [2009], Gold Nanorods: From Synthesis and Properties to Biological and Biomedical Applications, *Advanced Materials*, Vol. 21, No. 48, pp 4880.

Jain, P. K. & El-Sayed, M. A. [2008], Surface Plasmon Coupling and Its Universal Size Scaling in Metal Nanostructures of Complex Geometry: Elongated Particle Pairs and Nanosphere Trimers, *The Journal of Physical Chemistry C*, Vol. 112, No. 13, pp 4954-4960.

Jain, P. K., Lee, K. S., El-Sayed, I. H. & El-Sayed, M. A. [2006], Calculated Absorption and Scattering Properties of Gold Nanoparticles of Different Size, Shape, and Composition: Applications in Biological Imaging and Biomedicine, *The Journal of Physical Chemistry B*, Vol. 110, No. 14, pp 7238-7248.

Lee, K.-S. & El-Sayed, M. A. [2005], Dependence of the Enhanced Optical Scattering Efficiency Relative to That of Absorption for Gold Metal Nanorods on Aspect Ratio, Size, End-Cap Shape, and Medium Refractive Index, *The Journal of Physical Chemistry B*, Vol. 109, No. 43, pp 20331-20338.

Loo, C., Lowery, A., Halas, N., West, J. & Drezek, R. [2005], Immunotargeted Nanoshells for Integrated Cancer Imaging and Therapy, *Nano letters*, Vol. 5, No. 4, pp 709-711.

Mackey, M. A., Ali, M. R., Austin, L. A., Near, R. D. & El-Sayed, M. A. [2014], The Most Effective Gold Nanorod Size for Plasmonic Photothermal Therapy: Theory and in Vitro Experiments, *The Journal of Physical Chemistry B*, Vol. 118, No. 5, pp 1319-1326.

Mcpeak, K. M., Jayanti, S. V., Kress, S. J., Meyer, S., Iotti, S., Rossinelli, A. & Norris, D. J. [2015], Plasmonic Films Can Easily Be Better: Rules and Recipes, *ACS photonics*, Vol. 2, No. 3, pp 326-333.

Melancon, M. P., Lu, W., Yang, Z., Zhang, R., Cheng, Z., Elliot, A. M., Stafford, J., Olson, T., Zhang, J. Z. & Li, C. [2008], In Vitro and in Vivo Targeting of Hollow Gold Nanoshells Directed at Epidermal Growth Factor Receptor for Photothermal Ablation Therapy, *Molecular cancer therapeutics*, Vol. 7, No. 6, pp 1730-1739.

Nikoobakht, B., Wang, Z. & El-Sayed, M. [2000], Self-Assembly of Gold Nanorods, *The Journal of Physical Chemistry B*, Vol. 104, No. 36, pp 8635-8640.

Novo, C., Gomez, D., Perez-Juste, J., Zhang, Z., Petrova, H., Reismann, M., Mulvaney, P. & Hartland, G. V. [2006], Contributions from Radiation Damping and Surface Scattering to the Linewidth of the Longitudinal Plasmon Band of Gold Nanorods: A Single Particle Study, *Physical Chemistry Chemical Physics*, Vol. 8, No. 30, pp 3540-3546.

Ordal, M. A., Bell, R. J., Alexander, R. W., Long, L. L. & Querry, M. R. [1985], Optical Properties of Fourteen Metals in the Infrared and Far Infrared: Al, Co, Cu, Au, Fe, Pb, Mo, Ni, Pd, Pt, Ag, Ti, V, and W, *Applied optics*, Vol. 24, No. 24, pp 4493-4499.

Perenboom, J. a. a. J., Wyder, P. & Meier, F. [1981], Electronic Properties of Small Metallic Particles, *Physics Reports*, Vol. 78, No. 2, pp 173-292.

Pérez-Juste, J., Pastoriza-Santos, I., Liz-Marzán, L. M. & Mulvaney, P. [2005], Gold Nanorods: Synthesis, Characterization and Applications, *Coordination Chemistry Reviews*, Vol. 249, No. 17–18, pp 1870-1901.

Sun, Z., Ni, W., Yang, Z., Kou, X., Li, L. & Wang, J. [2008], Ph‐Controlled Reversible Assembly and Disassembly of Gold Nanorods, *Small*, Vol. 4, No. 9, pp 1287-1292.

Vartia, O. S., Ylä-Oijala, P., Markkanen, J., Puupponen, S., Seppälä, A., Sihvola, A. & Ala-Nissila, T. [2016], On the Applicability of Discrete Dipole Approximation for Plasmonic Particles, *Journal of Quantitative Spectroscopy and Radiative Transfer*, Vol. 169, No. pp 23-35.

Vollmer, M. & Kreibig, U. [1995], *Optical Properties of Metal Clusters*,

Wang, J., Dong, B., Chen, B., Jiang, Z. & Song, H. [2012], Selective Photothermal Therapy for Breast Cancer with Targeting Peptide Modified Gold Nanorods, *Dalton Transactions*, Vol. 41, No. 36, pp 11134-11144.